



ELECTRONIC, THERMODYNAMIC PROPERTIES, NONLINEAR OPTICAL RESPONSES, AND MOLECULAR DOCKING STUDIES ON CEPHALEXIN

Tarun Chaudhary¹, Bhawani Datt Joshi²

¹Central Department of Physics, Tribhuvan University, Kirtipur, Kathmandu, Nepal

²Department of Physics, Tribhuvan University, Siddhanath Science Campus, Mahendranagar, 10406, Nepal

*Corresponding author: bhawani.joshi@snc.tu.edu.np, pbdjoshi@gmail.com

(Received: September 18, 2021; Revised: April 02, 2022; Accepted: May 26, 2022)

ABSTRACT

The topology analysis of electron localization function (ELF), localized orbital locator (LOL), the study of nonlinear optical properties, thermal properties, and biological activities of cephalaxin have been performed using DFT/B3LYP and employing 6-311++G(d,p) basis sets. The Mulliken atomic charge on atoms has been calculated. The quantities describing nonlinear optical (NLO) properties like molecular polarizability (α), first hyperpolarizability (β), and second hyperpolarizability (γ) were comparable to the values of urea. The computed value of the second hyperpolarizability was found to be negative, which is an important feature for the system of controllable NLO devices. The thermodynamic properties like heat capacity (S), enthalpy (H), and entropy (S) are positively correlated with the temperature. Further, the title molecule shows good potentiality for binding with the selected target protein matrix metalloproteinase-2.

Keywords: Cephalaxin, ELF, LOL, nonlinear optical properties, thermodynamics, molecular docking

INTRODUCTION

Cephalaxin, C₁₆H₁₇N₃O₄S, is an antibiotic from the first-generation cephalosporin (Nguyen and Graber, 2020). It is active against most gram-positive and many gram-negative bacteria (Speight *et al.*, 1972). Cephalaxin, a white to cream-colored crystalline powder, is stable below a mild acidic condition (Manelli, 1975). It is used to treat respiratory tract infections, Gonorrhoea, urinary tract infections, and several infections due to susceptible organisms (Bailey *et al.*, 1970; Speight *et al.*, 1972).

The recent work on cephalaxin reflects the DFT study on structural, chemical, and spectroscopic properties. Cephalaxin at normal temperature has two stable

conformers (Chaudhary *et al.*, 2021). Moreover, organic molecules exhibit significant non-linear optical properties (NLO) (Kariper, 2017) and compounds with nitrogen and Sulphur contribute to various biological activities (Joshi *et al.*, 2018). Thus, the present work deals with non-linear optical properties, topology analysis, thermal properties, and biological activities. The electron localization function (ELF) and localized orbital locator (LOL) have been plotted to depict the electron localization. The quantities like static dipole moment, molecular polarizability, first hyperpolarizability, and second hyperpolarizability have been calculated. Further, these properties are also compared with the value of standard, conventional molecule, urea.

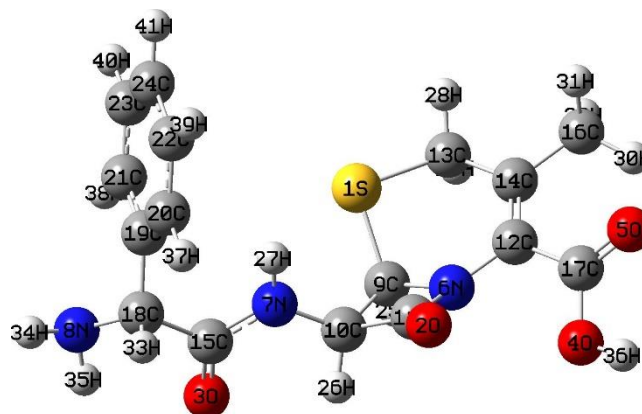


Figure 1 Optimized structure of cephalaxin.

The correlation of thermodynamic properties like heat capacity, enthalpy, entropy, and temperature is studied. Ultimately, the non-covalent interaction of cephalaxin

with matrix metalloproteinase-2 has been investigated using a molecular docking approach. The optimized structure of cephalaxin is shown in Fig. 1.

MATERIALS AND METHODS

Computational and theoretical details

The software package Gaussian 09 (Frisch *et al.*, 2009) was used for various computational studies in the present work. The density functional theory (DFT) using the B3LYP exchange correlation function with a basis set 6-311++(d,p) has been used for the calculation (Becke, 1993; Parr, 1980). Further, GaussView 05 (Dennington *et al.*, 2009) was used for visualizing the optimized structure of the title molecule. The topology study, Electron Localization Function (ELF), and Localized Molecular Orbital (LOL) have been performed using Multiwfn 3.4.1 software (Lu and Chen, 2012). The ELF function is defined by the equation (Silvi & Savin, 1994; Yang, 2010).

$$\text{ELF} = \frac{1}{1 + \left(\frac{D}{D_h}\right)^2} \quad (1)$$

$$\text{With } D = \frac{1}{2} \sum_i |\nabla \varphi_i|^2 - \frac{1}{8} \frac{|\nabla \rho|^2}{\rho}$$

$$\text{and } D_h = \frac{3}{10} (3\pi^2)^{2/3} \rho^{5/3}$$

Where, D and D_h represent excess kinetic energy and reference value, respectively.

The molecular polarizability, electric dipole moment, first hyperpolarizability, and second hyperpolarizability have been computed using a finite field approach employing a 6311++G(d,p) basis set. Using the finite field, the energy in the static electric field is expanded in terms of the Taylor's series (Kumar *et al.*, 2017).

$$E(F) = E(0) - \sum_i \mu_i F_i - \frac{1}{2} \sum_{i,j} \alpha_{ij} F_i F_j - \frac{1}{6} \sum_{i,j,k} \beta_{ijk} F_i F_j F_k - \frac{1}{24} \sum_{i,j,k,l} \gamma_{ijkl} F_i F_j F_k F_l \dots \quad (2)$$

Here, $E(0)$ is the total energy in the absence of an electrical field, and the quantities μ_i , α_{ij} , β_{ijk} and γ_{ijkl} represent the dipole moment, the polarizability, the first hyperpolarizability, and the second hyperpolarizability, respectively. The subscripts i, j, k, and l represent the Cartesian coordinates. The subscripts i, j, k, and l represent the Cartesian coordinates. The total static dipole moment (μ_0), mean polarizability ($|\alpha_0|$), anisotropy of polarizability ($\Delta\alpha$), first hyperpolarizability (β_0), and second hyperpolarizability (γ_0) that describe the non-linear optical phenomena of the molecule can be determined by the equations (Kumar *et al.*, 2017; Joshi *et al.*, 2013) as follows:

$$\mu_0 = (\mu_x^2 + \mu_y^2 + \mu_z^2)^{1/2} \quad (3)$$

$$|\alpha_0| = \frac{1}{3} (\alpha_{xx} + \alpha_{yy} + \alpha_{zz}) \quad (4)$$

$$\Delta\alpha = 2^{-1/2} \left[(\alpha_{xx} - \alpha_{yy})^2 + (\alpha_{yy} - \alpha_{zz})^2 + (\alpha_{zz} - \alpha_{xx})^2 + 6\alpha_{xx}^2 \right]^{1/2} \quad (5)$$

$$\beta_0 = \left[(\beta_{xxx} + \beta_{xyy} + \beta_{xzz})^2 + (\beta_{yyy} + \beta_{xxy} + \beta_{yzz})^2 + (\beta_{zzz} + \beta_{xxz} + \beta_{yyz})^2 \right]^{1/2} \quad (6)$$

$$\gamma_0 = \frac{1}{5} [\gamma_{xxxx} + \gamma_{yyyy} + \gamma_{zzzz} + 2(\gamma_{xxyy} + \gamma_{yyzz} + \gamma_{zzxx})] \quad (7)$$

The dipole moment, molecular polarizability, first hyperpolarizability, and second hyperpolarizability are first rank (vector), second rank, third rank, and fourth rank tensors, respectively.

The Gaussian 09 at the B3LYP/6-311+G(d,p) level, has been used to compute thermodynamic quantities like entropy, heat capacity, and enthalpy in the gas phase. The thermodynamic contributions of translational motion, rotational motion, electronic motion, and vibrational motion are obtained in terms of the partition function, $q(V,T)$. The given equations (Ochterski, 2000) are used to determine the various thermodynamic quantities.

$$\text{Total entropy, } S_{\text{total}} = S_{\text{translational}} + S_{\text{rotational}} + S_{\text{vibrational}} + S_{\text{electronic}} \quad (8)$$

$$\text{Total internal energy, } E_{\text{total}} = E_{\text{translational}} + E_{\text{rotational}} + E_{\text{vibrational}} + E_{\text{electronic}} \quad (9)$$

$$\text{Total heat capacity, } C_{\text{total}} = C_{\text{translational}} + C_{\text{rotational}} + C_{\text{vibrational}} + C_{\text{electronic}} \quad (10)$$

$$\text{Corrected enthalpy, } H_{\text{corrected}} = E_{\text{total}} + k_B T \quad (11)$$

where, different entropy contributions from translational, rotational, vibrational and electronic motion are

$$S_{\text{translational}} = R \left(\ln q_t + 1 + \frac{3}{2} \right),$$

$$S_{\text{rotational}} = R \left(\ln q_r + \frac{3}{2} \right), S_{\text{vibrational}} =$$

$$R \sum_K \left(\frac{\theta_{v,K}/T}{e^{\theta_{v,K}/T} - 1} - \ln (1 - e^{-\theta_{v,K}/T}) \right)$$

$$\text{and } E_{\text{electronic}} = (\ln q_e + 0).$$

Similarly, internal thermal energy and heat capacity contributions due to different motions are

$$E_{\text{translational}} = \frac{3}{2} RT, \quad E_{\text{rotational}} = RT,$$

$$E_{\text{vibrational}} = R \sum_K \theta_{v,K}/T \left(\frac{1}{2} - \frac{1}{e^{\theta_{v,K}/T} - 1} \right)$$

$$\text{and } C_{\text{translational}} = \frac{3}{2} R, \quad C_{\text{rotational}} = R,$$

$$C_{\text{vibrational}} = R \sum_K \theta_{v,K}/T \left(\frac{\theta_{v,K}/T}{e^{\theta_{v,K}/T} - 1} \right)^2.$$

The electronic contribution term for both thermal energy and heat capacity is zero.

The study of intermolecular non-covalent interactions between target proteins and cephalixin, the flexible-rigid blind docking, has been performed using AutoDockVina software (Trott and Olson, 2010). The result of AutoDockVina has been visualized and interpreted with the help of bio visualizer software (Studio, 2009). Generally, the binding affinity of a docked complex is determined on the basis of the scoring function. The scoring function for AutoDockVina can be obtained using the equation (Tanchuk *et al.*, 2016).

$$\Delta G_{\text{binding}} = \Delta G_{\text{H-bond}} + \Delta G_{\text{hydrophobic}} + \Delta G_{\text{repulsion}} + \Delta G_{\text{gauss}} + \Delta G_{\text{AutoDock Vina score}} \quad (12)$$

where $\Delta G_{\text{H-bond}}$ represents the change in the binding energy due to hydrogen bond, $\Delta G_{\text{hydrophobic}}$, due to hydrophobic interaction, ΔG_{gauss} ($\text{gauss}_1(d) = e^{-(d/0.5)^2}$ and $\text{gauss}_2(d) = e^{-((d-3)/2)^2}$), due to steric effects, $\Delta G_{\text{repulsion}}$, due to repulsion and $\Delta G_{\text{AutoDock Vina score}}$, due to rotational bonds penalty.

RESULTS AND DISCUSSION

ELF and LOL

Electron localization function (ELF) and localized orbital locator (LOL) are described on the basis of electron density by Becke and Edgecombe (Becke and Edgecombe, 1990; Schmider and Becke, 2002). The ELF and LOL display similar interpretations, however, ELF is based on kinetic energy density and the LOL on

gradients of localized orbital locators (Chaudhary *et al.*, 2021). ELF measures Pauli repulsion effects (Abraham *et al.*, 2019).

The quantitative values of ELF and LOL come down in the range of 0-1 where the degree of localization for electrons is high for values greater than 0.5 and the degree of delocalization is high for the value less than 0.5 (Chaudhary *et al.*, 2021). The Multiwfn software has been used to plot the ELF and LOL maps of the title molecule. The ELF and LOL plot of the title molecule have been shown in Figs. 2 and 3. In the ELF and LOL, the red region represents the localized electrons, and the Blue region represents the delocalized electrons. The red zone between every two atoms represents the bond critical point (BCP).

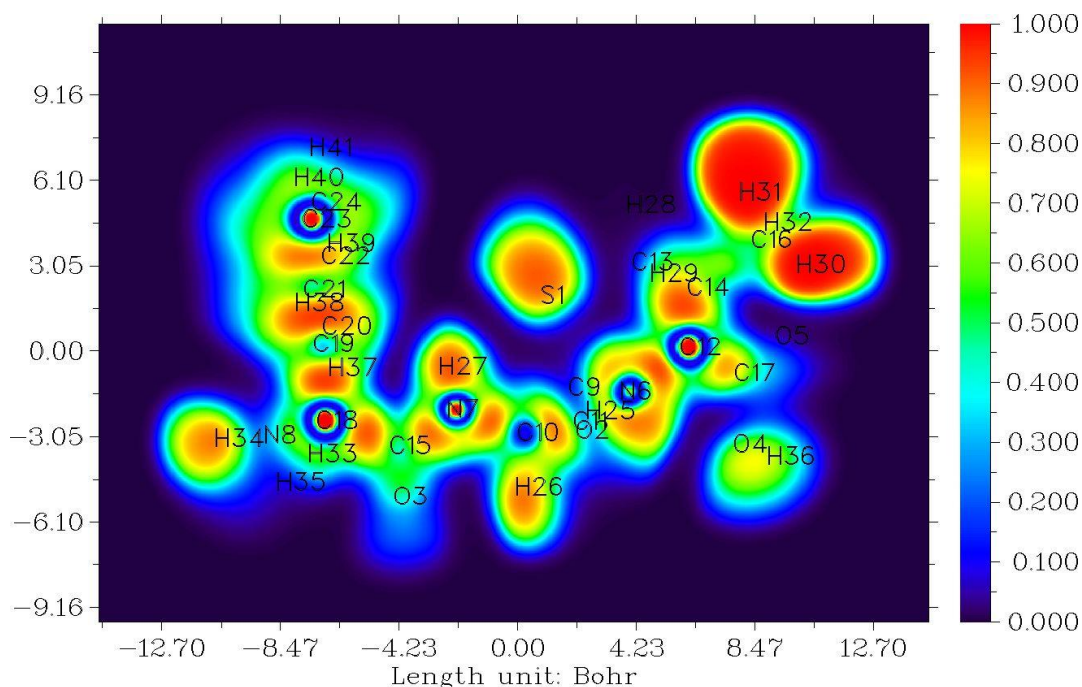


Figure 2 Electron localization function (ELF) of cephalixin.

The red zone across nitrogen and oxygen represents the lone pair associated with them. Similarly, high electron localization is depicted across hydrogen atoms due to maximum Pauli repulsion. On the other hand, a blue color zone is found across non-hydrogen heavy atoms. The blue color, at the center of the atoms, represents the atomic shell and the ring-like structures indicate the electron delocalization of electrons between core and valence electrons.

Mulliken charges

Mulliken population analysis is complementary to molecular electrostatic potential (MEP) and it provides the net atomic population in the molecule (Kumar *et al.*, 2017). Atomic charges affect different molecular properties, including dipole moment, polarizability and hyperpolarizability, and further help in understanding ionization potential and chemical potential (Abraham *et al.*, 2017). The Mulliken charge associated with various

atoms of cephalixin has been obtained using the B3LYP/6-311++G(d,p) level of theory. The calculated Mulliken charges of various atoms of the title compound is illustrated in Table 1 and presented by a simple bar diagram in Fig. 4. The atomic charge on all hydrogen atoms and atoms N6, N7, C9, C12, C14, C19, and C21 have positive charges (0.1596-0.5247|e|) and all the remaining atoms have negative charges. The carbon atom C13 has the highest magnitude of negative atomic charge (-0.9247|e|) since it is attached to less electronegative atom S1. The other atoms like O2, O3, O4, O5 have atomic charges in the range of -0.1704|e| to -0.3149|e| and N8 has -0.3104|e|. The net negative charge on oxygen atoms (electron donor) and the positive charge on hydrogen atoms have a significant role in intermolecular hydrogen bonding as observed in the section on molecular docking.

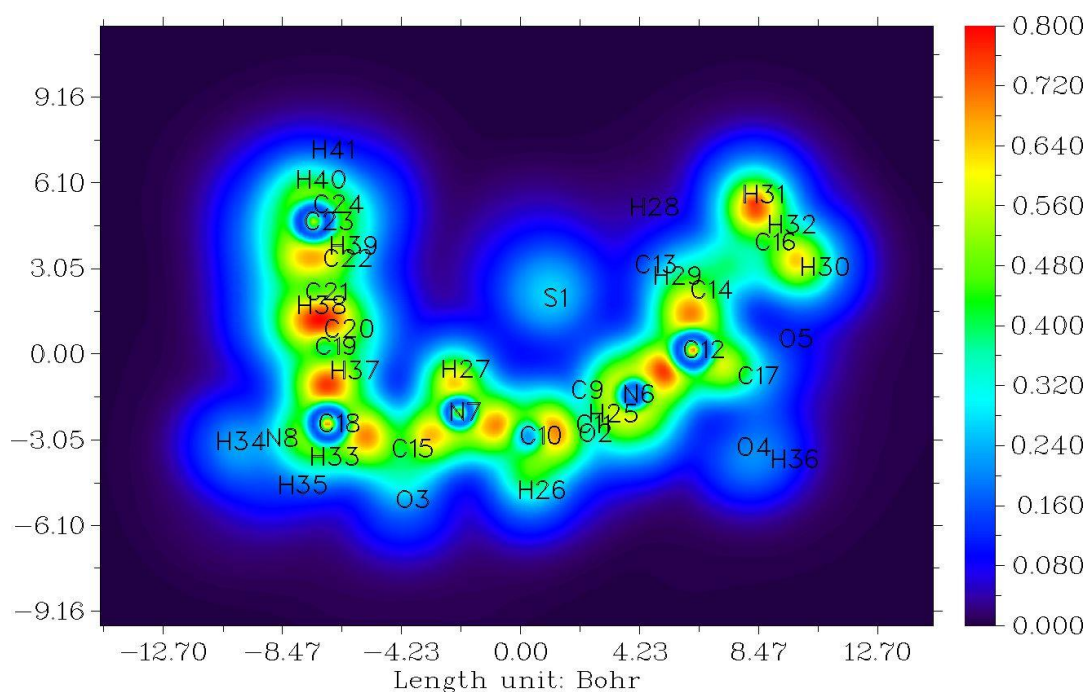


Figure 3 Orbital localization function (LOI) of cephalixin.

Mulliken population analysis is complementary to molecular electrostatic potential (MEP) and it provides the net atomic population in the molecule (Kumar *et al.*, 2017). Atomic charges affect different molecular properties, including dipole moment, polarizability and hyperpolarizability, and further help in understanding ionization potential and chemical potential (Abraham *et al.*, 2017). The Mulliken charge associated with various atoms of cephalixin has been obtained using the B3LYP/6-311++G(d,p) level of theory. The calculated Mulliken charges of various atoms of the title compound is illustrated in Table 1 and presented by a simple bar diagram in Fig. 4. The atomic charge on all hydrogen

atoms and atoms N6, N7, C9, C12, C14, C19, and C21 have positive charges (0.1596-0.5247|e|) and all the remaining atoms have negative charges. The carbon atom C13 has the highest magnitude of negative atomic charge (-0.9247|e|) since it is attached to less electronegative atom S1. The other atoms like O2, O3, O4, O5 have atomic charges in the range of -0.1704|e| to -0.3149|e| and N8 has -0.3104|e|. The net negative charge on oxygen atoms (electron donor) and the positive charge on hydrogen atoms have a significant role in intermolecular hydrogen bonding as observed in the section on molecular docking.

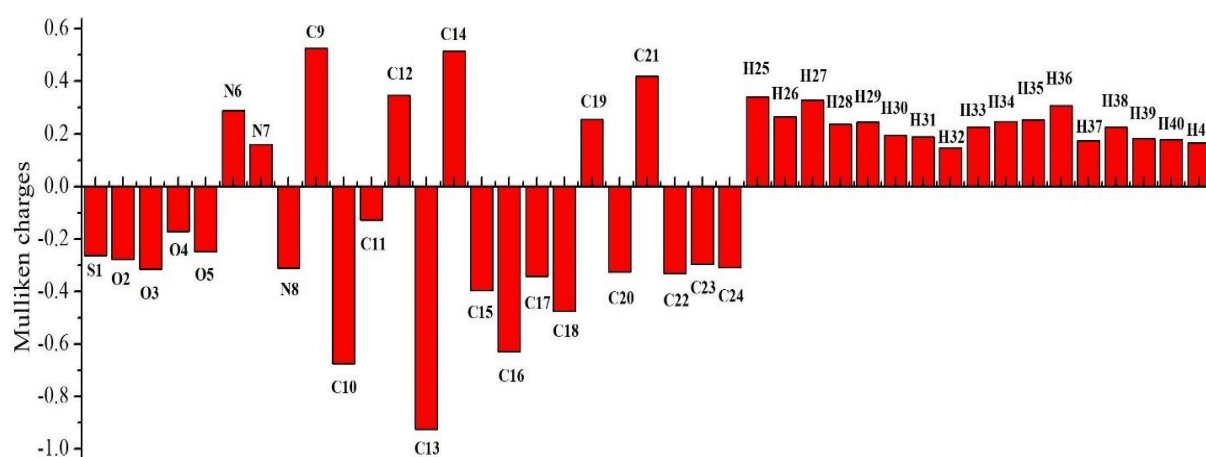


Figure 4 Calculated Mulliken charges of cephalixin.

Table 1: Mulliken charges calculated at B3LYP/6-311++G(d,p) level of theory.

Atom	Charges e	Atom	Charges e	Atom	Charges e	Atom	Charges e
S 1	-0.2627	C 12	0.3474	C 23	-0.2968	H 34	0.2467
O 2	-0.2766	C 13	-0.9247	C 24	-0.3093	H 35	0.2539
O 3	-0.3149	C 14	0.5152	H 25	0.3406	H 36	0.3076
O 4	-0.1704	C 15	-0.3956	H 26	0.2647	H 35	0.2539
O 5	-0.2480	C 16	-0.6283	H 27	0.3280	H 36	0.3076
N 6	0.2893	C 17	-0.3411	H 28	0.2361	H 37	0.1741
N 7	0.1596	C 18	-0.4754	H 29	0.2440	H 38	0.2266
N 8	-0.3104	C 19	0.2556	H 30	0.1944	H39	0.1815
C 9	0.5247	C 20	-0.3248	H 31	0.1888	H40	0.1780
C 10	-0.6755	C 21	0.4194	H 32	0.1468	H41	0.1664
C 11	-0.1275	C 22	-0.3326	H 33	0.2252		

NLO properties

The nonlinear optics, in the presence of electromagnetic fields give rise to new magnetic fields with different frequency, phase and other physical properties (Joshi *et al.*, 2013). The energy of the system in the presence of an electric field is the function of the electric fields (Issaoui *et al.*, 2015). The delocalization of π electrons in the molecule deals with the NLO properties of the system (Kariper, 2017). In the last few years, NLO properties have been of great interest due to their potential applications in telecommunication, data storage, optical signal processing, etc. (Koparir, 2013; Joshi, 2016). The dipole moment (μ_0), mean polarizability $|\alpha_0|$, anisotropy of polarizability ($\Delta\alpha$), first hyperpolarizability (β_0), and second hyperpolarizability (γ_0) of cephalixin are illustrated in Table 2. The calculated value of μ_0 , $|\alpha_0|$, $\Delta\alpha$, β_0 , and γ_0 are 3.1362 Debye, 3.1362 Debye, 21.4940

$\times 10^{-24}$ esu, 36.0946 $\times 10^{-24}$ esu, 0.4440 $\times 10^{-30}$ esu and -0.12849×10^{-35} esu. Urea is the standard, conventional molecule which is used to institute the threshold value for the comparative study of NLO properties of different molecules (Abraham *et al.*, 2017). The dipole moment of the title molecule is higher than the value of urea (1.3732 Debye). However, the first hyperpolarizability (β_0) is comparable to the value of urea (0.3728×10^{-30} esu), so the molecule exhibits significant NLO properties. On the other hand, the value of second hyperpolarizability (γ_0) is negative. In quantum optics, the negative value of γ_0 is very important because it causes a defocusing effect of an incident beam and such molecular systems can be good candidates for systems of controllable nonlinear properties (Nakano *et al.*, 1996; Kumar *et al.*, 2017).

Table 2: The calculated dipole moment (μ_0), mean polarizability $|\alpha_0|$, anisotropy of polarizability ($\Delta\alpha$) first hyperpolarizability (β_0), and second hyperpolarizability (γ_0) of cephalixin.

Dipole moment (Debye)	Polarizability (* 10^{-24} esu)	First Hyperpolarizability (* 10^{-30} esu)	Second hyperpolarizability (* 10^{-35} esu)
$\mu_x = 0.5882$	$\alpha_{xx} = -140.4955$	$\beta_{xxx} = 14.7286$	$\gamma_{xxxx} = -9060.7026$
$\mu_y = 2.9643$	$\alpha_{xy} = -2.4790$	$\beta_{xxy} = -40.9736$	$\gamma_{yyyy} = -2271.7508$
$\mu_z = -0.8380$	$\alpha_{yy} = -143.0230$	$\beta_{yyy} = 22.0851$	$\gamma_{zzzz} = -1421.9954$
$\mu_0 = 3.1362$	$\alpha_{xz} = -17.9694$	$\beta_{yyy} = 32.0184$	$\gamma_{xxyy} = -1683.9580$
$\mu_0(\text{Urea}) = 1.3732$	$\alpha_{yz} = -5.6946$	$\beta_{xxx} = -7.2215$	$\gamma_{xxzz} = -1756.0085$
	$\alpha_{zz} = -151.5867$	$\beta_{xyz} = -17.3457$	$\gamma_{yyzz} = -611.3782$
	$ \alpha_0 = 21.4940$	$\beta_{yyz} = 12.7285$	$\gamma_0 = -0.12849$
	$\Delta\alpha = 36.0946$	$\beta_{xzz} = 12.0654$	
	$\Delta\alpha(\text{Urea}) = 9.7710$	$\beta_{yzz} = 6.9303$	
		$\beta_{zzz} = 10.2229$	
		$\beta_0 = 0.4440$	
		$\beta_0(\text{Urea}) = 0.3728$	

Thermodynamic properties

The temperature has a direct effect on the chemical reactivity and the mechanism of drug action (Basha *et al.*,

2019; Choudhary *et al.*, 2014). The thermodynamic parameters are estimated from the Boltzmann distribution and partition function (Singh *et al.*, 2016). Thermodynamic properties like heat capacity, enthalpy,

entropy, zero-point energy, total energy, and rotational constant of cephalixin have been illustrated in Table 3. To study the thermal behavior of cephalixin, the temperature varied from 50 K to 600K, and the respective values of thermodynamic quantities are noted. Hence, the quadratic equations, from 13 to 15 have been obtained from the second-order polynomial fit between the thermodynamic quantities (a dependent variable) and the temperature (an independent variable). The graph showing quadratic fit in Fig. 5 demonstrates the positive correlation of enthalpy (H_m^o), heat capacity ($C_{p,m}^o$), entropy (S_m^o), and temperature. The value of R^2 for H_m^o , $C_{p,m}^o$ and S_m^o is obtained as 1, 0.9996, and 0.9994, respectively. The quantitative value of the thermodynamic parameters increases with the increase in temperature, which is due to the increase in vibrational motion with an increase in temperature. Furthermore, the specific heat capacity of the title compound at room temperature (298.15 K) has been calculated to be 1022.07J/kg-K (355.06 J/Mol-K), which is slightly

smaller than the value, 1322.77 J/kg-K of amino acid, glycine (Spink & Wadsö, 1975). However, the specific heat capacity of cephalixin is very close to the estimated value (960.36 J/kg-K) of a biologically active molecule, alkaloid aristolochic acid I (Joshi *et al.*, 2013).

$$H_m^o = 833.7112 + 0.0629T + 4.7996 \times 10^{-4}T^2 \quad (R^2 = 1) \quad (13)$$

$$C_{p,m}^o = 31.7992 + 1.2119T - 4.1214 \times 10^{-4}T^2 \quad (R^2 = 0.9996) \quad (14)$$

$$S_m^o = 269.5741 + 1.5674T - 5.1161 \times 10^{-4}T^2 \quad (R^2 = 0.9994) \quad (15)$$

The above equations can also be further utilized during the study of the interaction of the title molecule with another compound. They help to predict the Gibbs free energy and then the spontaneity of the reaction. In addition, these give useful details that can be used for the analysis of thermodynamic energies and can be used to estimate the direction of chemical reaction using the second law of thermodynamics in the thermochemical field (Joshi *et al.*, 2013).

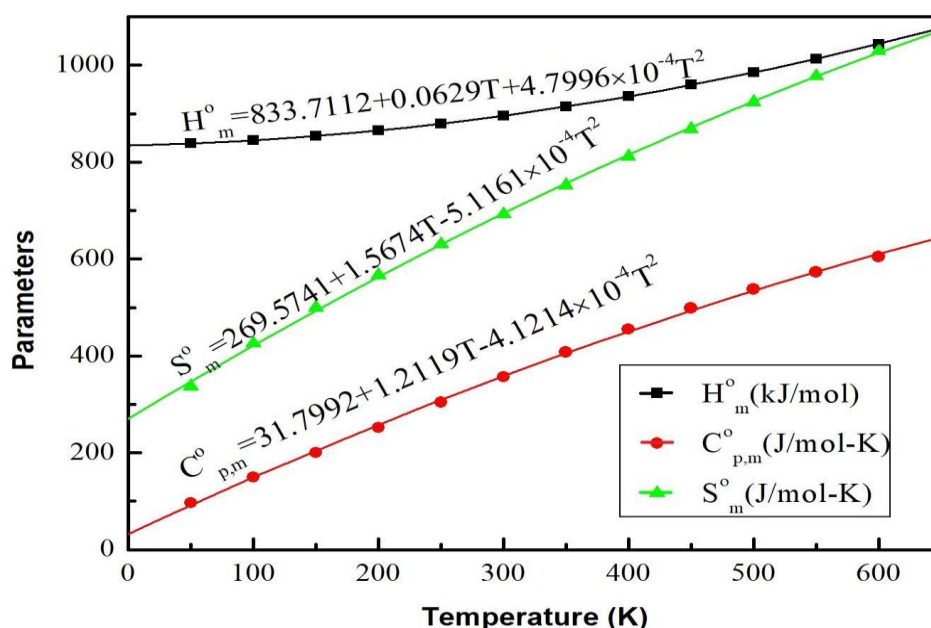


Figure 5 Correlation of enthalpy, heat capacity, entropy and temperature for cephalixin.

Table 3: Thermodynamic parameters of cephalixin at various temperature.

Temperature (K)	Enthalpy (kJ/mol)	Heat capacity (J/mol-K)	Entropy (J/mol-K)	Zero-point energy (Joules/mol)	Total energy (eV)
50	838.6870	97.00186	336.72	835576	-40371.2566
100	844.8877	149.9211	426.3036	835576.1	-40371.2566
150	853.6448	200.4513	500.0298	835576	-40371.2566
200	864.9458	251.7471	567.0743	835576.1	-40371.2566
250	878.8450	304.2981	630.7296	835576.1	-40371.2566
300	895.3760	356.8952	692.3934	835576.1	-40371.2566
350	914.5011	407.7141	752.5635	835574.9	-40371.2566
400	936.0947	455.2778	811.2483	835576	-40371.2566
450	959.9644	498.8081	868.4059	835576	-40371.2566
500	985.9052	538.0959	923.7895	835580.2	-40371.2566
550	1013.7037	573.3293	977.6627	835576.1	-40371.2566
600	1043.1758	604.8725	1029.641	835576.1	-40371.2566

Molecular docking

In medicinal chemistry, for entire potential drug targets, the study of drug-protein interaction can be performed either using an experimental method or a computational method. Molecular docking conducted on AutoDockVina is a popular computational technique that is used to calculate the quantitative parameters of ligand and protein interaction (Ferreira da Costa *et al.*, 2018). It helps to anticipate the binding mode and affinity between ligand and receptor protein interactions. In the present work, for the docking analysis, the target protein (matrix metalloproteinase-2) (MMP-2) has been predicted with the help of online software, the Swiss

Target Prediction (Daina *et al.*, 2019). The invasive features of certain human malignancies, such as colon and breast tumors, are influenced by matrix metalloproteinases (Kanayama *et al.*, 1998) MMP-2 has a key role in the pathophysiology of inflammatory and cancerous disorders in a variety of organs, including the lungs (Chakrabarti and Patel, 2005). Hence, docking analysis has been performed with this particular protein to know the biological activities of cephalexin with this protein. The PDB code was downloaded from the RSCB protein data bank (Rose *et al.*, 2010).

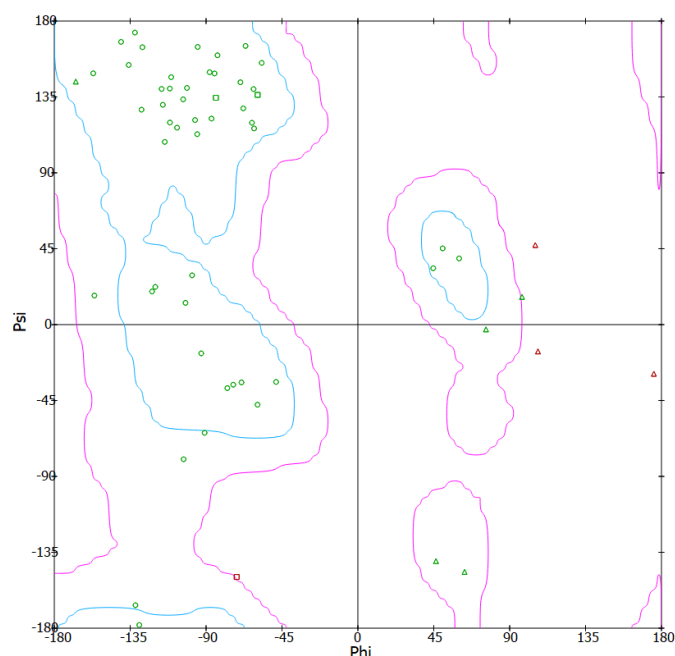


Figure 6 Ramachandran plots of protein 1J7M

The Ramachandran plots in Fig. 6 demonstrate the phi-psi torsional angles of the residues of the protein. It shows that maximum residues lie inside the blue line the allowed region. The ligand molecule cephalexin was prepared by optimizing it using Gaussian 09 at B3LYP/6-311++G(d,p) level. Thus, the most stable state corresponding to the minimum ground state energy is obtained. Water was removed and the polar hydrogen was added to the receptor protein with the help of AutoDock. A docking simulation has been formed using AutoDockVina. The Discovery studio was used to observe the ligand protein interactions. The center of the binding active sites is located at $x=-0.044$, $y=0.009$, $z=-0.151$ and it is limited in the grid box of size $40 \text{ \AA} \times 40 \text{ \AA} \times 40 \text{ \AA}$ of spacing 0.375 \AA . The docked structure of cephalexin-1J7M is presented in Fig. 7. The various

docking parameters are displayed in Table 4. The title molecule is strongly bound to the protein 1J7M protein with a binding affinity -5.9 kcal/mol . The electropositive atoms H35, H27, and the electronegative atom O2 interact non-covalently with residues GLU27, SER28, LYS25, and GLU27 of the proteins.

Thus, the formation of a total of four hydrogen bonds takes place and the length of these bonds falls in the range of 1.8814 \AA to 2.5723 \AA . Further, the root mean square deviation (RMSD) between the docked structure and its initial structure is less than 1.2 \AA which is less than 2 \AA . Hence, in general, cephalexin shows good binding activity with the protein matrix metalloproteinase-2 (PDB code: 1J7M).

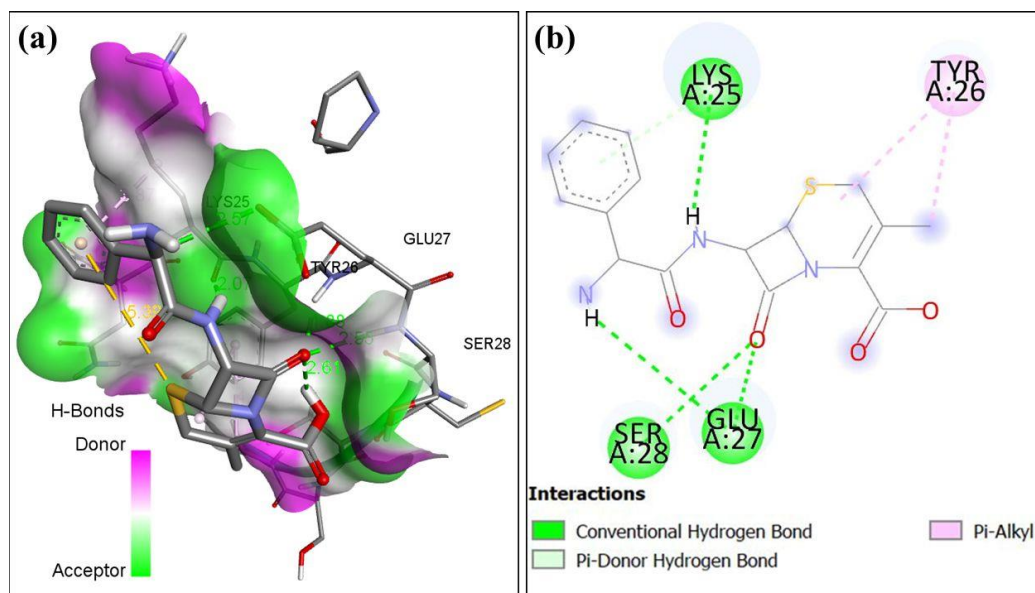


Figure 7 (a) Docked structure and (b) interactions of cephalixin with protein 1J7M.

Table 4: Docking parameters of cephalixin against the protein matrix metalloproteinase-2.

Protein	PDB code	Binding affinity (kcal/mol)	Bond length(Å)	H-Bonded Residues	Rmsdvalue (Å)	Inhibition constant (μ M)
Matrixmetalloproteinase-2	1J7M	-5.9	1.8814 2.5530 2.0745 2.5723	GLU27 SER28 LYS25 GLU27	1.2	47.06

CONCLUSIONS

In the present work, the analysis of electron localization function (ELF) and localized orbital locator (LOL) and non-linear optical properties, thermal properties, as well as biological activities of cephalixin has been performed using DFT/B3LYP employing 6-311++G(d,p) basis sets. The ELF and LOL map show that the localization of electrons is higher across oxygen, nitrogen and hydrogen, and carbon atoms. The calculated Mulliken atomic charges associated with carbon atoms C13 and C9 are found to be $-0.9247|e|$ and $0.5247|e|$, which are the highest negative charge and the highest positive charges, respectively. The nonlinear optical properties (NLO) have been computed. The estimated value of first hyperpolarizability (0.4440×10^{-30} esu) is comparable to the value of the standard molecule, urea. These properties represent the significant NLO properties. In addition, the molecule has negative second hyperpolarizability (-0.12849×10^{-35} esu) which is very important for constructing controllable NLO devices. Furthermore, the quadratic fits, demonstrating the nature of the correlation between enthalpy, heat capacity, entropy, and temperature, are useful for the thermodynamic energies analysis. Furthermore, the binding sites of the title molecule and the protein matrix metalloproteinase-2 have been predicted. The binding affinity of the protein-molecule complex was predicted to be -5.9 kcal/mol. Thus, the molecular docking study theoretically proves that the title molecule has a good binding potential against the protein 1J7M.

ACKNOWLEDGEMENTS

We sincerely acknowledge Prof. Poonam Tandon, HOD, Department of Physics, Lucknow University, India, for providing software facilities, including the Gaussian 09 program, as well as sharing research concepts during the whole study period.

AUTHOR CONTRIBUTIONS

Both authors contributed equally.

CONFLICT OF INTERESTS

The authors declare no conflict of interests.

DATA AVAILABILITY STATEMENT

The data that support the findings of this study are available from the corresponding author, upon reasonable request.

REFERENCES

- Abraham, C.S., Muthu, S., Prasana, J.C., Armaković, S., Armaković, S.J., & Geoffrey, B. (2019). Computational evaluation of the reactivity and pharmaceutical potential of an organic amine: A DFT, molecular dynamics simulations and molecular docking approach. *Spectrochimica Acta Part A: Molecular and Biomolecular Spectroscopy*, 222, 117-188.
- Abraham, C.S., Prasana, J.C., & Muthu, S. (2017). Quantum mechanical, spectroscopic and docking studies of 2-amino-3-bromo-5-nitropyridine by density functional method. *Spectrochimica Acta Part A: Molecular and Biomolecular Spectroscopy*, 181, 153-163.

- Bailey, A., Hadley, A., Walker, A., & James, D.G. (1970). Cephalaxina new oral antibiotic. *Postgraduate Medical Journal*, 46(533), 157.
- Basha, S.J., Chamundeeswari, S.V., Muthu, S., & Raajaraman, B. (2019). Quantum computational, spectroscopic investigations on 6-aminobenzimidazole by DFT/TD-DFT with different solvents and molecular docking studies. *Journal of Molecular Liquids*, 296, 111787.
- Becke, A.D. (1993). A new mixing of hartree-fock and local density-functional theories. *The Journal of Chemical Physics*, 98(2), 1372-1377.
- Becke, A.D., & Edgecombe, K.E. (1990). A simple measure of electron localization in atomic and molecular systems. *The Journal of Chemical Physics*, 92(9), 5397-5403.
- Chakrabarti, S., & Patel, K.D. (2005). Matrix metalloproteinase-2 (MMP-2) and MMP-9 in pulmonary pathology. *Experimental Lung Research*, 31(6), 599-621.
- Chaudhary, T., Chaudhary, M.K., & Joshi, B.D. (2021). Topological and reactivity descriptor of carisoprodol from DFT and molecular docking approach. *Journal of Institute of Science and Technology*, 26(1), 74-82.
- Choudhary, N., Agarwal, P., Gupta, A., & Tandon, P. (2014). Quantum chemical calculations of conformation, vibrational spectroscopic, electronic, NBO and thermodynamic properties of 2, 2-dichloro-n-(2, 3-dichlorophenyl) acetamide and 2, 2-dichloro-n-(2, 3-dichlorophenyl) acetamide. *Computational and Theoretical Chemistry*, 1032, 27-41.
- Daina, A., Michielin, O., & Zoete, V. (2019). Swiss Target Prediction: updated data and new features for efficient prediction of protein targets of small molecules. *Nucleic Acids Research*, 47(W1), W357-W364.
- Dennington, R., Keith, T., & Millam, J. (2009). GaussView, version 5.
- Ferreira da Costa, J., Silva, D., Caamaño, O., Brea, J.M., Loza, M.I., Munteanu, C.R., Pazos, A., García-Mera, X., & González-Díaz, H. (2018). Perturbation theory/machine learning model of chembl data for dopamine targets: docking, synthesis, and assay of new l-prolyl-l-leucyl-glycinamide peptidomimetics. *ACS Chemical Neuroscience*, 9(11), 2572-2587.
- Frisch, M., Trucks, G., Schlegel, H.B., Scuseria, G.E., Robb, M.A., Cheeseman, J.R., Scalmani, G., Barone, V., Mennucci, B., Petersson, G., et al. (2009). Gaussian 09, revision d. 01, Gaussian. NC., Wallingford CT, 201.
- Issaoui, N., Ghalla, H., Muthu, S., Flakus, H., & Oujia, B. (2015). Molecular structure, vibrational spectra, AIM, HOMO-LUMO, NBO, UV, first order hyperpolarizability, analysis of 3-thiophenecarboxylic acid monomer and dimer by hartree-fock and density functional theory. *Spectrochimica Acta Part A: Molecular and Biomolecular Spectroscopy*, 136, 1227-1242.
- Joshi, B.D. (2016). Chemical reactivity, dipole moment and first hyperpolarizability of aristolochic acid I. *Journal of Institute of Science and Technology*, 21(1), 1-9.
- Joshi, B.D., Khadka, J.B., & Bhatt, A. (2018). Structure, electronic and vibrational study of 7-methyl-2, 3-dihydro-(1, 3) thiazolo (3, 2-a) pyrimidin-5-one by using density functional theory. *Journal of Institute of Science and Technology*, 22(2), 1-11.
- Joshi, B.D., Srivastava, A., Gupta, V., Tandon, P., & Jain, S. (2013). Spectroscopic and quantum chemical study of an alkaloid aristolochic acid I. *Spectrochimica Acta Part A: Molecular and Biomolecular Spectroscopy*, 116, 258-269.
- Kanayama, H.O., Yokota, K.Y., Kurokawa, Y., Murakami, Y., Nishitani, M., & Kagawa, S. (1998). Prognostic values of matrix metalloproteinase-2 and tissue inhibitor of metalloproteinase-2 expression in bladder cancer. *Cancer: Interdisciplinary International Journal of the American Cancer Society*, 82(7), 1359-1366.
- Kariper, S.E. (2017). Spectroscopic and quantum chemical studies on some β -lactam inhibitors. *Turkish Computational and Theoretical Chemistry*, 1(2), 13-26.
- Koparir, M. (2013). 7, 7-bis [(aza-18-crown-6) carbonyl] thioindigo: Synthesis, experimental, theoretical characterization and biological activities. *Medicine Science*, 2(1), 386-402
- Kumar, A., Kumar, R., Gupta, A., Tandon, P., & D'silva, E.D. (2017). Molecular structure, nonlinear optical studies and spectroscopic analysis of chalcone derivative (2e)-3-[4-(methylsulfanyl) phenyl]-1-(3-bromophenyl) prop-2-en-1-one by DFT calculations. *Journal of Molecular Structure*, 1150, 166-178.
- Lu, T., & Chen, F. (2012). Multiwfn: a multifunctional wavefunction analyzer. *Journal of Computational Chemistry*, 33(5), 580-592.
- Manelli, L.P. (1975). Cephalaxin. In *Analytical profiles of drug substances* (Vol. 4, pp. 21-46). Academic Press.
- Nakano, M., Kiribayashi, S., Yamada, S., Shigemoto, I., & Yamaguchi, K. (1996). Theoretical study of the second hyperpolarizabilities of three charged states of pentalene. a consideration of the structure-property correlation for the sensitive second hyperpolarizability. *Chemical Physics Letters*, 262(1-2), 66-73.
- Nguyen, H.M., & Graber, C.J. (2020). A critical review of cephalaxin and cefadroxil for the treatment of acute uncomplicated lower urinary tract infection in the era of bad bugs, few drugs. *International Journal of Antimicrobial Agents*, page 106085.
- Ochterski, J.W. (2000). Thermochemistry in gaussian. *Gaussian Inc*, 1, 1-19.
- Parr, R.G. (1980). Density functional theory of atoms and molecules. In *Horizons of Quantum Chemistry*, pages 5-15. Springer.
- Rose, P.W., Beran, B., Bi, C., Bluhm, W.F., Dimitropoulos, D., Goodsell, D.S., Pri'c, A., Quesada, M., Quinn, G.B., Westbrook, J.D., et al. (2010). The RSCB protein data bank: redesigned web site and web services. *Nucleic Acids Research*, 39(suppl 1), D392-D401.
- Schmider, H.L., & Becke, A.D. (2002). Two functions of the density matrix and their relation to the chemical bond. *The Journal of Chemical Physics*, 116(8), 3184-3193.

- Silvi, B., & Savin, A. (1994). Classification of chemical bonds based on topological analysis of electron localization functions. *Nature*, 371(6499), 683-686.
- Singh, S., Singh, H., Karthick, T., Agarwal, P., Erande, R. D., Dethle, D. H., & Tandon, P. (2016). Combine experimental and theoretical investigation on an alkaloid–dimethylisoborreverine. *Journal of Molecular Structure*, 1103, 187-201.
- Speight, T., Brogden, R., & Avery, G. (1972). Cephalixin: a review of its antibacterial, pharmacological and therapeutic properties. *Drugs*, 3(1), 9-78.
- Spink, C.H., & Wadsö, I. (1975). Thermochemistry of solutions of biochemical model compounds. 4. The partial molar heat capacities of some amino acids in aqueous solution. *The Journal of Chemical Thermodynamics*, 7(6), 561-572.
- Studio, D. (2009). version 2.5. *Accelrys Inc.: San Diego, CA, USA*.
- Tanchuk, V.Y., Tanin, V.O., Vovk, A.I., & Poda, G. (2016). A new, improved hybrid scoring function for molecular docking and scoring based on autodock and autodockvina. *Chemical Biology and Drug Design*, 87(4), 618-625.
- Trott, O., & Olson, A.J. (2010). Autodockvina: improving the speed and accuracy of docking with a new scoring function, efficient optimization, and multithreading. *Journal of Computational Chemistry*, 31(2), 455-461.
- Yang, Y. (2010). Hexacoordinate bonding and aromaticity in silicon phthalocyanine. *The Journal of Physical Chemistry A*, 114(50), 13257-13267.